# Seismic velocity inversion using the FO-CRS stack in layered medium

Marcelo J. L. Mesquita (UFPA), João C. R. Cruz (UFPA), Alexandre S. Fernandes (UFPA), Raphael Di Carlo. S. dos Santos (UFPA/UFOPA), Diogo P. Rezende (UFPA)



## Abstract

**The development of seismic exploration depends strongly on the accurate determination of the subsurface velocity field. The estimate of velocities and depths in a geological environment is an important stage in processing and interpretation of seismic data. In this paper, we present a methodology based on the coherency inversion method. It consists to maximize a semblance function calculated from pre-stack seismic data, in order to obtain information about the velocities in the subsurface. We obtain the traveltime stack curve using the FO-CRS (finite-offset common-reflection-surface) approach for the CMP (common-mid-point) gather, whose parameters we obtain by ray tracing in the guess velocity model. By scanning the velocity for each layer in a given interval, we determine the optimum value based on the semblance criterion. We analyze the sensitivity of the semblance object function with respect to the lateral variation of the geological structure. The results obtained with noisy synthetic data show values very close to those adopted in the model, indicating the reliability of the FO-CRS approach in this inversion process.**

## Introduction

The estimate of velocities and depths is an important stage in the processing and interpretation of seismic data. In recent years, we have an increasing application of the full waveform inversion method (TARANTOLA, 1984). Nevertheless, it is very sensitive to the chosen initial velocity model. In this sense, the seismic tomography approaches continues to be an essential alternative to start the accurate velocity inversion. The two main ones are: (a) traveltime tomography (GOLDIN, 1979) and (b) non-linear coherence optimization (LANDA et al., 1989). In practice, the first has as disadvantage the needing of correct picking of events in the pre-stack data.

To overcome this problem, LANDA et al. (1988) have proposed a coherency inversion method that does not depend on pre-stack time picking and does not use on curves fitting. By the method, we have an optimization algorithm to produce a velocity model that maximizes some measure of coherence calculated from unstacked traces (common-shotpoint or common-midpoint) within a window along the traveltime curves. Ray tracing in the geologic model calculates these traveltime curves. Splines functions represent positions of the interfaces and interval velocities in the layers defined by points of the nodes.

A problem with this method is that the ray tracing calculates the traveltimes for all traces at each iteration, which is not computationally effective. To increase the computational effectiveness, we suggest use the FO-CRS method (GARABITO et al, 2011; ZHANG et al, 2001) to estimate the times from a single central ray tracing to each CMP gather.

In this paper, we present a study about the sensitivity of the semblance function in respect to the FO-CRS traveltimes approximation method in different estimated velocity models. We applied the method in noisy synthetic data from a geologic model with two curved interfaces. The results showed good approximations of the values adopted in the true model.

## Methodology

The method used involves the application of various techniques as shown in the flowchart of the Figure 1.

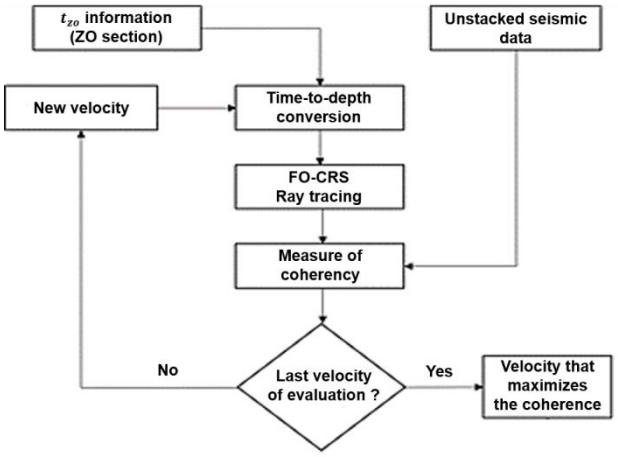


Figure 1: Flowchart of the analysis used on this paper.

In the first step, we obtain the traveltimes from picking of main events in the stacked section (zero-offset (ZO) section) to obtain the shape of the reflector, and to have the traveltimes of the normal rays.

The second step consists of the time-to-depth conversion of stacked seismic data using ray tracing with normal incidence (PEREYRA, 1987). We convert each selected point to a specific value of depth according to the selected velocity within a range stated for testing. After conversion, we interpolate the points using the cubic splines method, resulting in the reflecting interface.

The third step consists of the FO-CRS central ray tracing in order to calculate the traveltimes in the velocity model estimated in the previous step. BORTFELD (1989) and ZHANG et al. (2001) developed a 2-D hyperbolic traveltime approximation for paraxial rays in the vicinity of a central ray considering a finite offset between sources and receivers. For a central ray that starts at S, reflect at R on a reflector in subsurface, and emerges at the surface in G, the traveltime of the finite-offset paraxial ray, the so-called FO-CRS traveltime approximation, is given by

$$t^2(\nabla x_m, \nabla h) = \left[t_0 + \left(\frac{\operatorname{sen}\beta_G}{v_G} + \frac{\operatorname{sen}\beta_S}{v_S}\right)\nabla x_m + \left(\frac{\operatorname{sen}\beta_G}{v_G} - \frac{\operatorname{sen}\beta_S}{v_S}\right)\nabla h\right]^2 + t_0\left[(4K_1 - 3K_3)\frac{(\cos\beta_G)^2}{v_G} - K_2\frac{(\cos\beta_S)^2}{v_S}\right]\nabla x_m^2 + t_0\left[K_3\frac{(\cos\beta_G)^2}{v_G} - K_2\frac{(\cos\beta_S)^2}{v_S}\right]\nabla h^2 + 2t_0\left[K_3\frac{(\cos\beta_G)^2}{v_G} + K_2\frac{(\cos\beta_S)^2}{v_S}\right]\nabla x_m \nabla h \ , \quad (1)$$

where, $t_0$ is the traveltime along the central ray, $\beta_S$ and $\beta_G$ are the start and emergence angles of the central ray in the position of the source $S$ and the receiver $G$ with coordinates $x_S$ and $x_G$, respectively. The displacements $\nabla x_m = x_m - x_0$ and $\nabla h = h - h_0$ correspond to the midpoint and half-offset displacements where, $x_0 = (x_G + x_S)/2$ is the midpoint and $h_0 = (x_G - x_S)$ is the half-offset of the central ray with finite-offset. The midpoint $x_m$ and the half-offset $h$ are the coordinates of an arbitrary paraxial ray with finite-offset. The wave velocity at the source $S$ and receiver $G$ is given by $v_S$ and $v_G$, respectively. The quantities, $K_1$, $K_2$ and $K_3$ are the wavefront curvatures associated to the central ray and are calculated in the respective emergence points (GARABITO et al., 2011).

The FO-CRS traveltime approximation, defined in equation (1), simulates common-offset (CO) sections from multi-coverage pre-stack seismic data. For each sampled point $P_0(x_0, h_0, t_0)$ in the CO simulated section, there is a stacking surface defined by five parameters (Figure 2). The seismic events contained on this surface are summed, and the result is assigned to the given point $P_0$.

For CMP case, the source and the paraxial receiver, $\bar{S}$ and $\bar{G}$ are located symmetrically in relation to their corresponding points $S$ and $G$, in the central ray. Considering that the common midpoint is common to the central and paraxial rays, the CMP condition implies $\nabla x_m = 0$, and FO-CRS traveltime approximation (for diffraction or reflection), becomes (GARABITO et al, 2011.):

$$t^2(\nabla h) = \left[t_0 + \left(\frac{\operatorname{sen}\beta_G}{v_G} - \frac{\operatorname{sen}\beta_S}{v_S}\right)\nabla h\right]^2 + t_0\left[K_3\frac{(\cos\beta_G)^2}{v_G} - K_2\frac{(\cos\beta_S)^2}{v_S}\right]\nabla h^2. \quad (2)$$

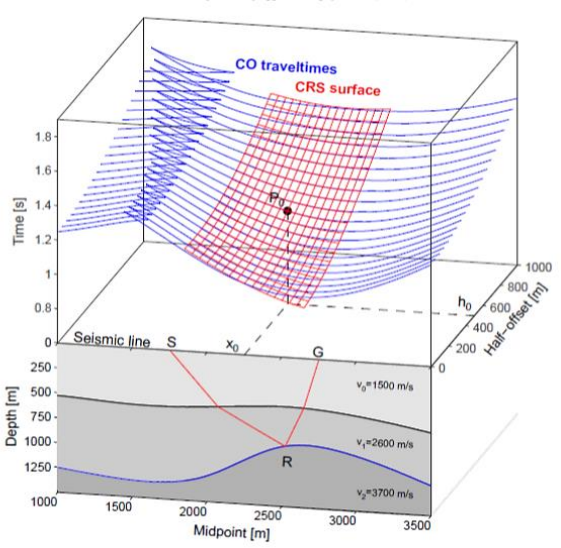


Figure 2: At the bottom, the representation of a 2-D geological model with three homogeneous layers separated by two curved and smooth interfaces. Notice the finite offset central ray, wherein $x_0$ is the midpoint and $h_0$ is the half-offset. At the top, traveltime curves related to the first reflections of the second interface (blue) with the FO-CRS traveltime approximation (red) associated to $P_0$ coordinate (GARABITO et al., 2011).

The fourth step consists of the coherency measure calculation. Coherency measures quantitatively express the similarity between multichannel data. Redundant signals in the channels may be measured, enhanced, extracted, adjusted or ignored. (NEIDELL & TANER, 1971).

Consider a coherency measure $E$. For all the shots (or midpoints) and reflectors, we can calculate the measure of total coherency over the traveltimes calculated by the FO-CRS approximation. The higher the sum of coherency, the better the interpretative model considered. Therefore, the inversion goals to find a model where this measure is maximum.

Let us adopt the semblance function (NEIDELL & TANER, 1971) to estimate the presence or absence of signals correlated along the traveltime curves calculated by FO-CRS method. The function $E$, that varies between 0 and 1, is given by:

$$E = \frac{1}{n}\frac{\left(\sum_t \sum_i A_{i,t}\right)^2}{\sum_t \sum_i (A_{i,t}^2)} \ . \quad (3)$$

In the equation (3), $n$ is the number of traces in the CMP gather (pre-stacked section) and $A_{i,t}$ is the amplitude value at the $i$-th trace at time $t$.

We repeat the process until the last scan velocity. We obtain the maximum semblance when the correct velocity is used, because it converts the events of the stacked section for the correct depth, approaching the true FO-CRS parameters and producing the best traveltime curve. In summary, the FO-CRS parameters depend on the chosen velocity.

**Example**

We applied the tests considering a geological model (Figure 3) with three homogeneous and isotropic layers. The acoustic velocities are $v_1 = 2000\,(m/s)$, for the first layer, and $v_2 = 2500\,(m/s)$ for the second, and $v_3 = 3000\,(m/s)$ for the last. We modeled using ray tracing method.

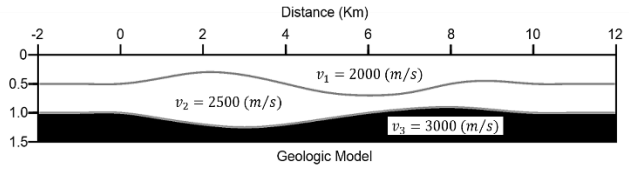


Figure 3: Velocity model with three homogeneous and isotropic layers.

In the acquisition, we used the split-spread array with 200 shots, spaced 50 m each, from 0 km to 9.95 km and 60 geophones, spaced 50 m each, covering the range from -1475 to 11425m. Once finished the conventional processing, we have a stacked section in time with 458 traces (458 CMPs). We added noise to traces with signal-to-noise ratio (snr) = 10.

We estimate the traveltimes of normal rays from the picking in the main events on the stacked section (Figure 4). The points selected have interval of 30 traces. The velocities used in the analysis are from 1500 m/s to 2500 m/s for the first layer, with steps of 10 m/s, and from 2000 m/s to 2750 m/s for the second layer, with steps of 50 m/s. Each velocity generates a model with the interface positioned at a different depth. We applied this inversion technique to the first and second layers.

We analyzed Six CMPs along each layer: 60, 120, 180, 240, 300, and 360. The criteria for selection the estimated velocities in layers is based on greatest value of semblance compared to other CMPs.

The total gap for each CMP is 1475 m, with 15 shots (from midpoint to the left) and 15 geophones (from midpoint to right). The FO-CRS central ray chosen is the one generated by the central source and geophone (central trace in the window).

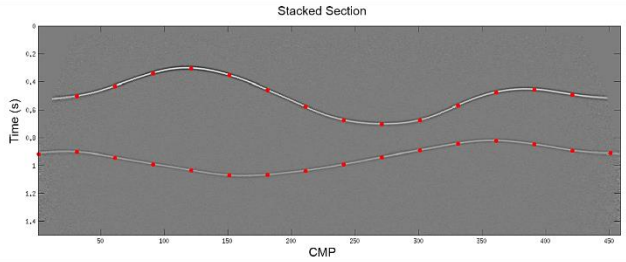


Figure 4: Stacked section and pickings points showing the normal ray traveltimes in main two events.

**Results**

For all CMPs analyzed in each layer, we obtained a seismic velocity, described in Table 1. Obeying the selection criteria, we chose the CMP 240 for the two layers, as it showed the highest value of semblance.

Table 1: True velocities for the two layers and estimated velocities for all CMPs in each layer.

| True Velocity (m/s) | Estimated Velocity (CMP 60) | Estimated Velocity (CMP 120) | Estimated Velocity (CMP 180) |
|---|---|---|---|
| $v_1$ = 2000 | 1980 (m/s) | 1980 (m/s) | 2480 (m/s) |
| $v_2$ = 2500 | 2000 (m/s) | 2350 (m/s) | 2500 (m/s) |
| **True Velocity (m/s)** | **Estimated Velocity (CMP 240)** | **Estimated Velocity (CMP 300)** | **Estimated Velocity (CMP 360)** |
| $v_1$ = 2000 | 1970 (m/s) | 1980 (m/s) | 1980 (m/s) |
| $v_2$ = 2500 | 2500 (m/s) | 2450 (m/s) | 2550 (m/s) |

For the first layer, CMP 240 showed the highest value of semblance, $E = 0.9377$, for $v_1 = 1970\,(m/s)$ estimated. The second highest semblance value was found for CMP 120, $E = 0.8669$, for$v_1 = 1980\,(m/s)$. Figures 5 and 6 show the velocity-semblance curves emphasizing the maximum semblance values and the best velocities in CMPs 240 and 180. Figure 7 shows the FO-CRS traveltime curve (red curve) and the pre-stacked data (CMP 240 – layer 1).

For the second layer, CMP 240 showed again the highest value of semblance, $E = 0.9067$, for $v_2 = 2500\,(m/s)$ estimated. The second highest semblance value was found for CMP 360, $E = 0.7134$, for $v_2 = 2550\,(m/s)$. Figures 8 and 9 show the velocity-semblance curves emphasizing the maximum semblance values and the best velocities in CMPs 240 and 360. Figure 10 shows the FO-CRS traveltime curve (red curve) and the pre-stacked data (CMP 240 – layer 2).

The last test was the evaluation of the velocity model that generated the best FO-CRS curves. Tables 2 and 3 show the real and estimated values of the velocities and depths of models for CMP 240 – layer 1 and CMP 240 – layer 2.

The estimated parameters presented very close values compared to the true model. The biggest misfit among the

estimated depths was 65 m. The velocities estimated were very close to the true ones.

The results showed a strong dependence of the FO-CRS curve in relation of the velocity model. If the model is wrong, the FO-CRS parameters calculated by the central ray will be wrong, and the traveltime curve is not satisfactory, resulting in a low semblance.

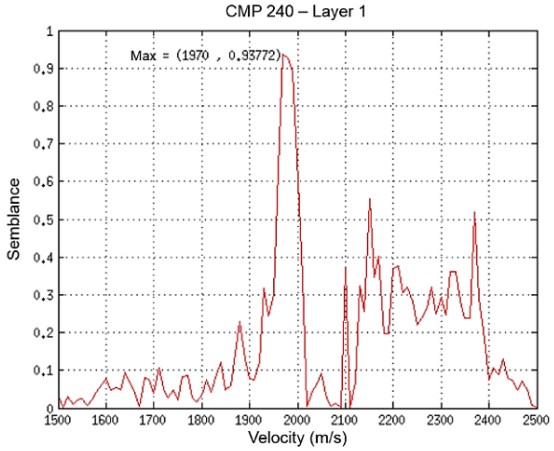


Figure 5: Velocity-semblance curve for CMP240 – layer 1, emphasizing the maximum semblance value and the best velocity. The correct velocity estimates correct depth of the interface, which contributes to the best FO-CRS traveltime curve, where the coherency is maximum.

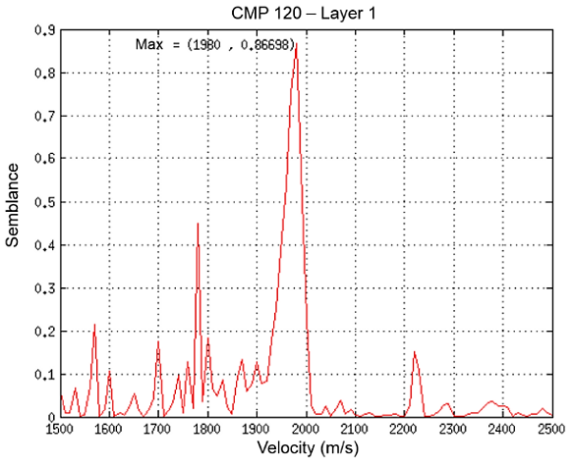


Figure 6: Velocity-semblance curve for CMP 120 – layer 1, emphasizing the maximum semblance value and the best velocity.

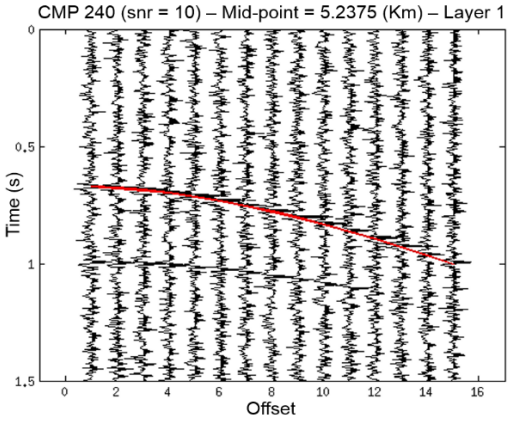


Figure 7: FO-CRS traveltime curve (red) for CMP 240 – layer 1 (snr=10). The traveltime of the central ray is on the trace 8.

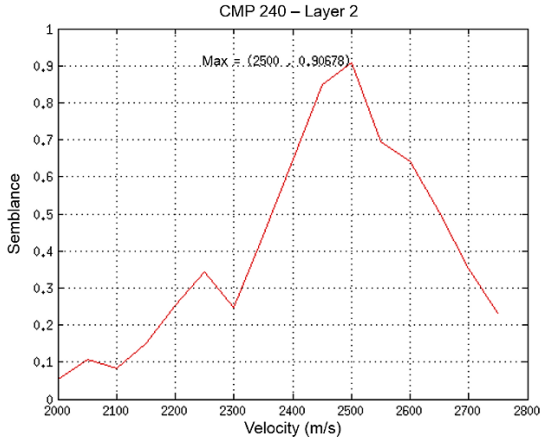


Figure 8: Velocity-semblance curve for CMP 240 – layer 2. Notice the maximum value of semblance and ideal velocity.

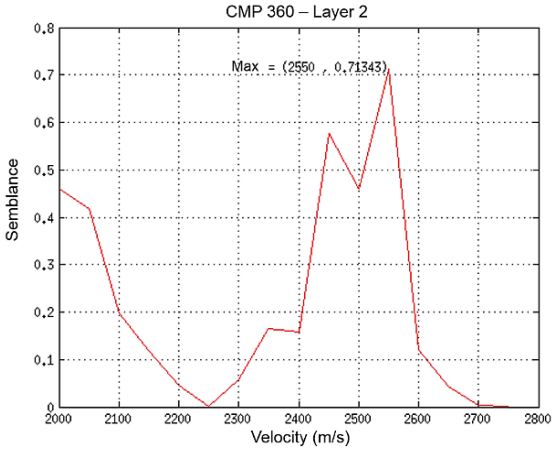


Figure 9: Velocity-semblance curve for CMP 360 – layer 2. Notice the maximum value of semblance and ideal velocity.

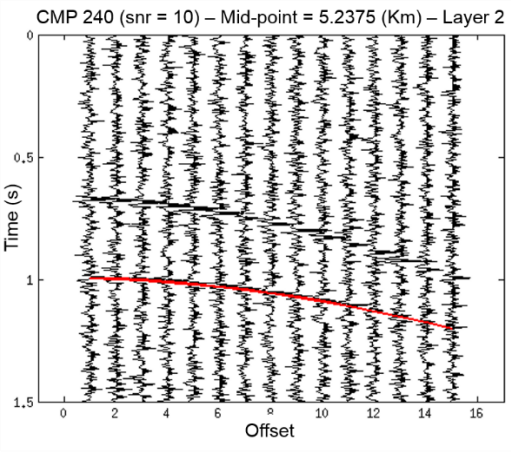


Figure 10: FO-CRS traveltime curve (red) for CMP 240 – layer 2 (snr=10). The traveltime of the central ray is on the trace 8.

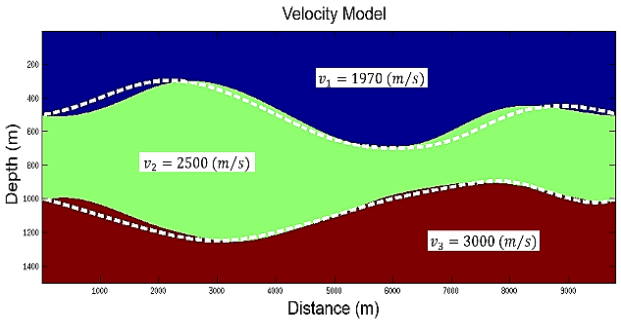


Figure 11: Velocity model estimated with optimum velocity obtained for the CMP 240 – layer 1 and CMP 240 – layer 2. The true synthetic model is shown as dashed lines.

Table 2: True parameters and estimated parameters considering the best velocity for maximum semblance in CMP 240 – layer 1.

| **True Parameters** | | **Estimated Parameters** | | **Misfit** |
|---|---|---|---|---|
| $X\ (m)$ | $Z\ (m)$ | $X\ (m)$ | $Z\ (m)$ | $Z\ (m)$ |
| 0 | 500 | 0 | 504 | +4 |
| 1000 | 400 | 1000 | 465 | + 65 |
| 2000 | 300 | 2000 | 327 | + 27 |
| 3000 | 350 | 3000 | 318 | -32 |
| 4000 | 500 | 4000 | 462 | - 38 |
| 5000 | 650 | 5000 | 633 | -17 |
| 6000 | 700 | 6000 | 692 | - 8 |
| 7000 | 650 | 7000 | 594 | -56 |
| 8000 | 500 | 8000 | 454 | - 46 |
| 9000 | 450 | 9000 | 471 | +21 |
| 10000 | 500 | 10000 | 504 | - 4 |
| $v_1 = 2000$ (m/s) | | $v_1 =1970$ (m/s) | | - 30 (m/s) |

Table 3: True parameters and estimated parameters considering the best velocity for maximum semblance in CMP 240 – layer 2.

| **True Parameters** | | **Estimated Parameters** | | **Misfit** |
|---|---|---|---|---|
| $X\ (m)$ | $Z\ (m)$ | $X\ (m)$ | $Z\ (m)$ | $Z\ (m)$ |
| 0 | 1000 | 0 | 1012 | +12 |
| 1000 | 1100 | 1000 | 1035 | - 65 |
| 2000 | 1200 | 2000 | 1165 | -35 |
| 3000 | 1250 | 3000 | 1248 | -2 |
| 4000 | 1200 | 4000 | 1214 | + 14 |
| 5000 | 1100 | 5000 | 1102 | + 2 |
| 6000 | 1000 | 6000 | 977 | -23 |
| 7000 | 930 | 7000 | 913 | - 17 |
| 8000 | 900 | 8000 | 912 | + 12 |
| 9000 | 1000 | 9000 | 984 | - 16 |
| 10000 | 1000 | 10000 | 1019 | +19 |
| $v_2 = 2500$ (m/s) | | $v_2 =2500$ (m/s) | | 0 (m/s) |

## Conclusions

The coherency inversion method seeks to maximize a coherency measure calculated in pre-stack traces along the traveltime curves estimated by ray tracing in the model.

This work proposed analyze the behavior of the semblance function with respect to the calculated traveltime curves using the FO-CRS method and its parameters as a function of the velocity used in the seismic estimated model. The main advantage is the better computational efficiency, because only a single ray (central ray) is traced.

The FO-CRS method was suitable for calculations required in the semblance maximization and in the optimization processes. The estimated parameters fitted with low error the true parameters of the synthetic model.

It is important to note the behavior of semblance function in presence of noise in high degree in trace gathers. Studies with others coherence measure methods are necessary in order to solve this kind of problem.

## Ackowledgementes

The authors would like to thank the *Programa de Pós-Graduação em Geofísica - Universidade Federal do Pará*, Geophysics network of PETROBRAS, and CAPES for the support.

## References

BORTFELD, R. Geometrical ray theory: rays and traveltimes in seismic systems (second order approximation of the traveltimes). Geophysics 1, 342-349, 1989.

GARABITO, G.; OLIVA, P. C.; CRUZ, J. C. R. Numerical analysis of the finite-offset common-reflection-traveltime approximations. Journal of Applied Geophysics, n. 74, p. 89-99, 2011.

GOLDIN, S. V. Interpretation of seismic data. Nedra, Moscow (in Russian), 1979. English translation: Seismic translation inversion, 1986. SE8, Tulsa.

LANDA, E.; KOSLOFF, D.; KEYDAR, S.; KOREN, Z.; RESHEF, M. A method for determination of velocity and depth from seismic reflection data. Geophysical Prospecting, 36, p. 223-243, 1988.

LANDA, E.; BEYDOUN, W.; TARANTOLA, A. Reference velocity model estimation from prestack waveforms: Coherency optimization by simulated annealing. Geophysics, v.54, n. 8, p. 984-990, 1989.

NEIDELL, N. S.; TANER, M. T. Semblance and other coherency measures for multichannel data. Geophysics, v. 36, p. 482-497, 1971.

PEREYRA, V. Modeling with ray tracing in two-dimensional curved homogeneous layered media. Micro-computer in Large Scale Scientific Computation, SIAM Pub. P. 39-67, 1987.

TARANTOLA, A. Inversion of seismic reflection data in the acoustic approximation. Geophysics, v. 49, 1259-1266, 1984.

RUBRAL, P. Common-Reflection-Surface (CRS) stack for common-offset. Geophys. Prospect, v. 49, 709-718, 2001.